

Paint with Music

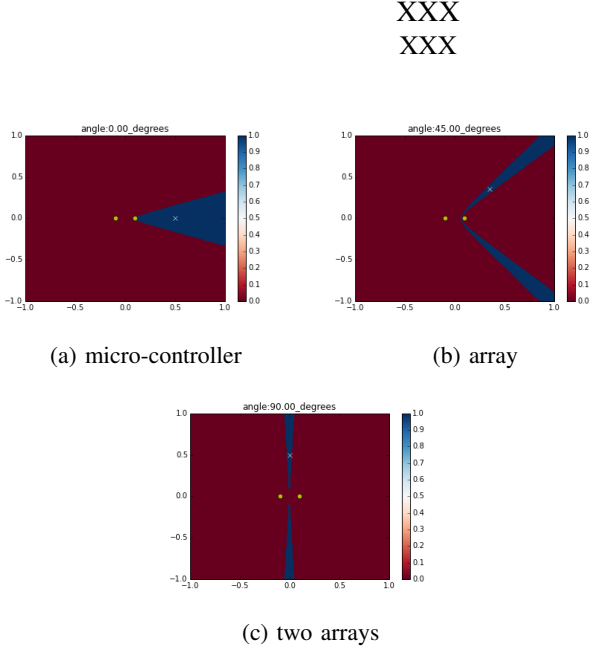


Fig. 1: Localization arrays

Abstract—The abstract goes here.

I. INTRODUCTION

II. PRIOR WORK

III. SIMULATION

In a 2D region, points with the same TDOA to two fixed locations form a hyperbola. However, in practical systems, we can only measure TDOA up to a precision. Therefore we look at all points with difference of distance close to some target value within measurement error ϵ . This ϵ represents accuracy on measurement of difference of distances, and in practice it is related to sampling rate and TDOA methods.

To see how precision affects localization accuracy, we simulated two microphones placed at: $M_1 : (x = -10\text{cm}, y = 0\text{cm})$ and $M_2 : (x = 10\text{cm}, y = 0\text{cm})$. A test sound source is emitted at point P 50 centimeters away from $(0, 0)$. Fig 1 shows the region where all points \hat{P} satisfy:

$$|(\hat{P}M_1 - \hat{P}M_2) - (PM_1 - PM_2)| < 1\text{cm}$$

Intuitively, points in the region have difference of distance very similar to each other. From fig 1, the region still has the shape of a hyperbola, but with an uncertainty region around the curve. The uncertainty region is not uniform around the curve, the farther away the point is, the larger the uncertainty region becomes. It indicates that the same delta distance movement will generate smaller difference of distance when

XXX
XXX

you are farther away from the array. The size of the uncertainty region is also angle dependent: points closer to the line of microphones have larger region compared to points close to the line perpendicular to microphones.

With more than two multiple microphones, each pair of microphones generates a hyperbolic region and localization becomes finding the intersection of regions. The smaller the intersection region, the better the localization accuracy. To see how accuracy changes with array placement and sound source location, three microphones are placed at three vertices of an 20cm equilateral triangle. An audio source is placed at 20 cm away from the center of the array. Fig 2 shows the intersection of regions for 5 different placement of the sound source. It can be seen that accuracy is worse when sound source is close to the line of any two microphones. This observation is consistent with two microphone case, since points close to line of microphones have a larger uncertainty region.

To see how sound source distance affects localization accuracy, the same simulation is carried out with sound source moved from 20cm to 80cm away from the center of the array. Results are presented in fig 3. Comparing with fig 2, accuracy decreases with distance to the array. This is also consistent with our observation in 2 microphone case where source farther away would result in larger uncertainty region.

Intersection area is a measure of the localization accuracy. To evaluate an array's accuracy in a region, we can place sound source at predetermined grid points in the region and look at the intersection area for each point in the grid. Results for a few different configurations are presented in fig 4.

Fig 4a shows the accuracy when microphones are placed at three vertices of a 20 cm equilateral triangle. The region inside the array has good accuracy. However, for regions along line of any two microphones, the accuracy drops significantly.

To evaluate how adding one microphone (without increasing array size) improves accuracy, another microphone is added to the array at $(0, 0)$. Result is presented in fig 4b. Addition of the new microphone only slightly improved the accuracy around the array region. Regions near lines of microphones still have significantly larger uncertainty region.

To evaluate array size's impact on accuracy, the size of original array from fig 4a is increased by a factor of 2. The result is presented in fig 4c. The overall uncertainty area decreased across the region.

In fig 4d, three microphones 10cm apart from each other are placed in a line on x-axis. The result indicates that this configuration has high uncertainty in nearly all regions except for regions near the microphones. In fig 4e, four microphones are placed at four corners of the region. Accuracy is consistently

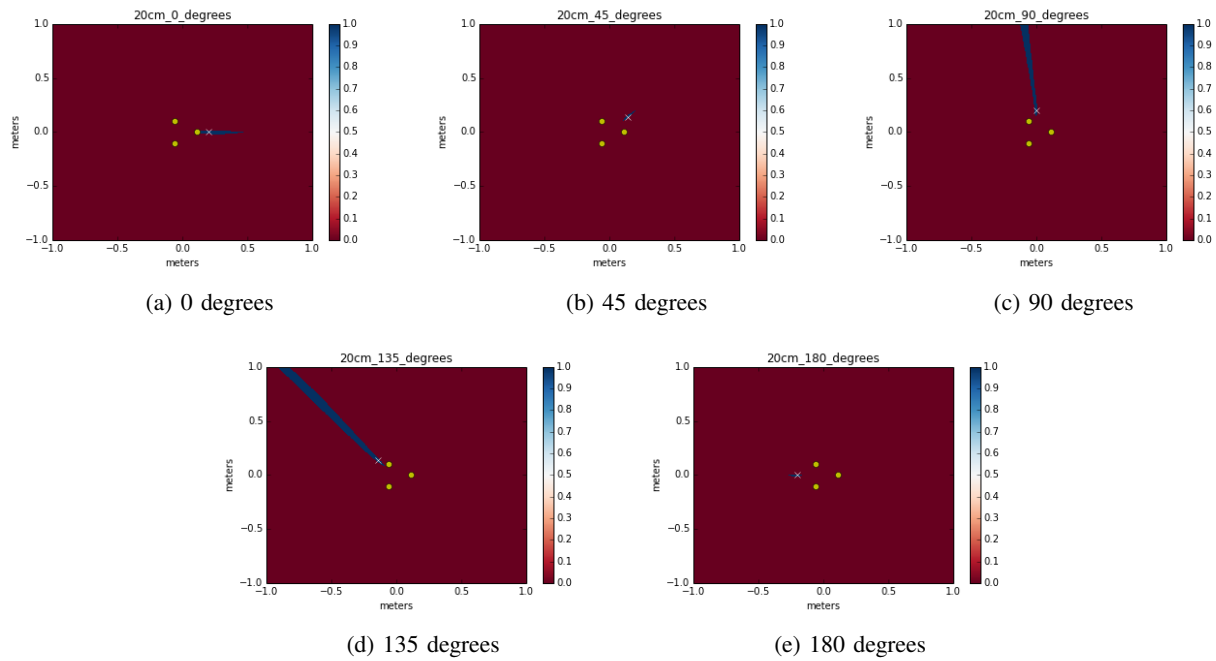


Fig. 2: 20cm equilateral triangle array. Source is 20cm away from the array

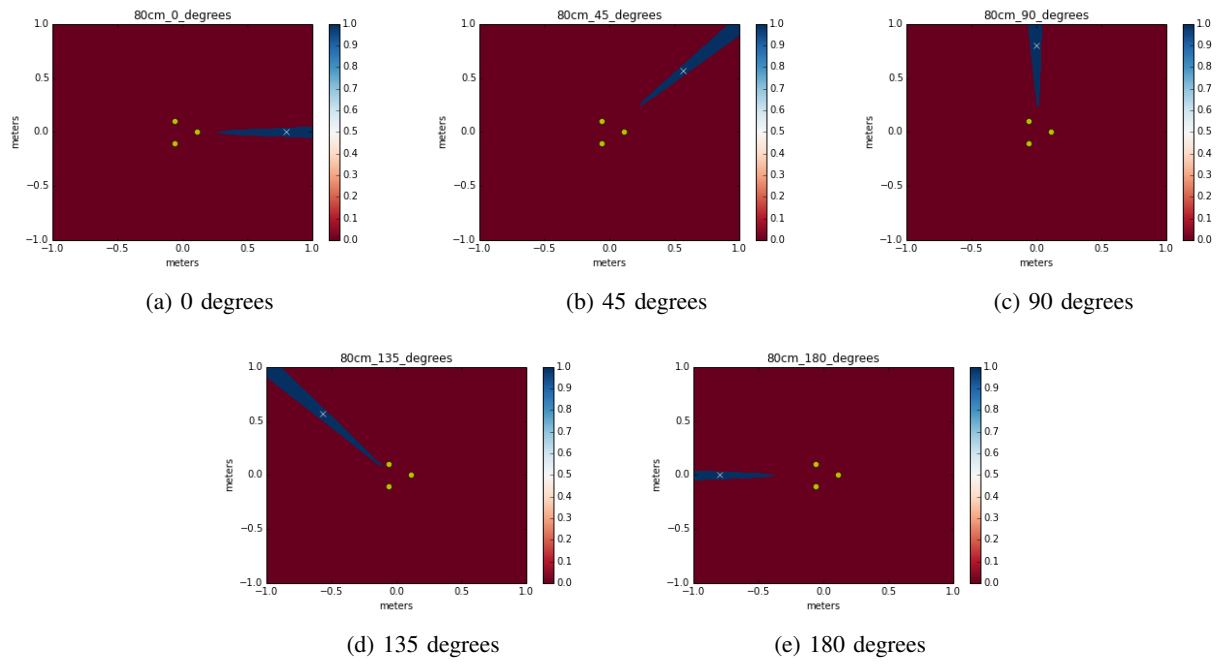


Fig. 3: 20cm equilateral triangle array. Source is 80cm away from the array

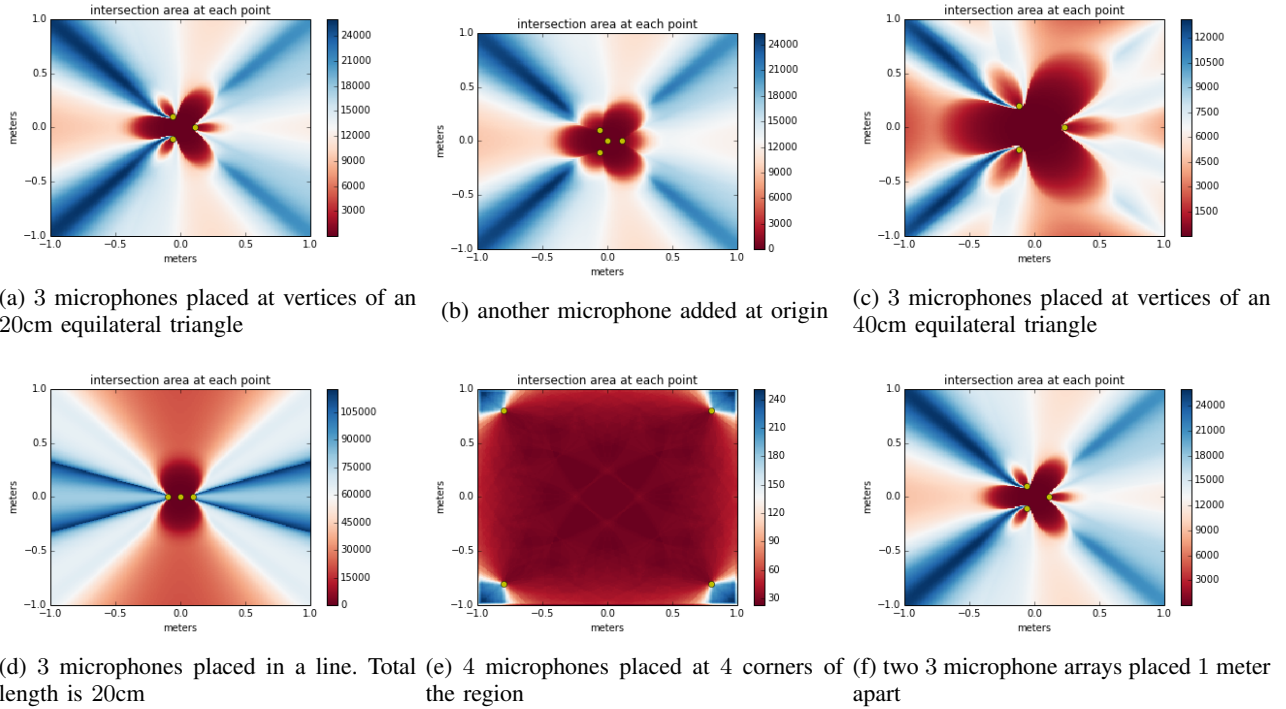


Fig. 4: Accuracy for different array configurations

good across the region. However, this configuration requires microphone to be placed far apart.

To get benefit of far away microphone placement without incurring overhead of placing individual microphones, two array solutions are explored. Fig 4f shows the accuracy map when two 3 microphone array are placed 1 meter apart. It shows that the array has good accuracy inside a one meter by one meter region

IV. SOUND LOCALIZATION

Points with the same time difference of arrival(TDOA) to two fixed points on a plane form a hyperbola. Since TDOA from each pair of microphones gives a hyperbola in the plane, localization becomes finding intersection of hyperbolas when more than two microphones are used. Localization relies on accurate estimate of delay differences between microphones.

Generalized Cross Correlation(GCC) provides a framework to estimate delay differences t_0 between two signals $x_1(t)$ and $x_2(t)$:

$$t_0 = \arg \max_{\tau} R_{x_1 x_2}(\tau) \quad (1)$$

$$R_{x_1 x_2}(\tau) = \int_{-\infty}^{\infty} W(\omega) X_1(\omega) X_2^*(\omega) e^{j\omega\tau} d\omega \quad (2)$$

, where $X_1(\omega)$ and $X_2(\omega)$ are Fourier Transform of $x_1(t)$ and $x_2(t)$. $W(\omega)$ provides a way to prefilter signals passed to cross correlation estimator. We experimented with three ways of prefiltering the signal:

GCC

$W(\omega) = 1$. No prefiltering is done. This is normal cross correlation.

GCC_PHAT

GCC_PHAT_SQRT

$W(\omega) = \frac{1}{|X_1(\omega)X_2^*(\omega)|}$. Each frequency is divided by its magnitude. Only phase information contributes to delay estimation.

$W(\omega) = \frac{1}{|X_1(\omega)X_2^*(\omega)|^{0.5}}$. This is somewhere between GCC and GCC_PHAT. part of magnitude information is included in delay estimation.

V. SYSTEM

The system uses two arrays, each with three microphones mounted on vertices of a 20cm equilateral triangle. A micro-controller is also attached to one of the vertices. Fig 5 shows a picture of the array setup. Micro-controller used in this project is *teensy 3.1*. It has 64k RAM memory and the ADC is capable of sampling at 500kHz. In this project, the micro-controller collects microphone data on all three channels for 12 millisecond and then send the recorded data to a computer through USB port for localization.

To speed up computation for real time localization, instead of searching for t_0 that maximizes equation 1, a grid search in 2D grid is performed. For each point in the grid, the theoretical TDOA to each microphone pair can be precomputed. Then localization resolves to calculating GCC for each microphone pair and performing a lookup for each point in the grid. To further improve localization accuracy, instead of using point estimate for TDOA, a likelihood map is built. Each entry in GCC output is used as the likelihood for that delay. With three microphones m_1, m_2, m_3 , there are three microphone pairs:

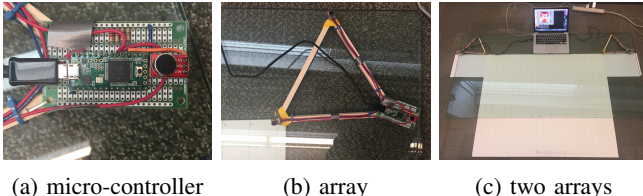


Fig. 5: Localization arrays

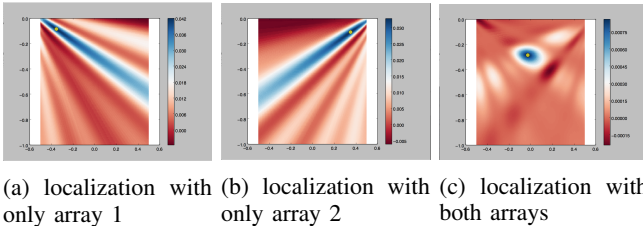


Fig. 6: Likelihood maps for localizing point at $(0.0, -0.3)$ m

m_1m_2, m_1m_3, m_2m_3 . Theoretical TDOA from each location (x, y) to each microphone pair is precomputed and stored in $D_{m_1, m_2}(x, y)$, $D_{m_1, m_3}(x, y)$, and $D_{m_2, m_3}(x, y)$. Then the likelihood map can be built as:

$$L(x, y) = R_{m_1, m_2}(D_{m_1, m_2}(x, y)) + R_{m_1, m_3}(D_{m_1, m_3}(x, y)) + R_{m_2, m_3}(D_{m_2, m_3}(x, y))$$

, where $R_{m_1, m_2}(\tau), R_{m_1, m_3}(\tau)$, and $R_{m_2, m_3}(\tau)$ denote GCC output from microphone pairs m_1m_2, m_1m_3 , and m_2m_3 .

Likelihood maps from two arrays can be combined into final likelihood map:

$$L(x, y) = L_1(x, y)L_2(x, y) \quad (3)$$

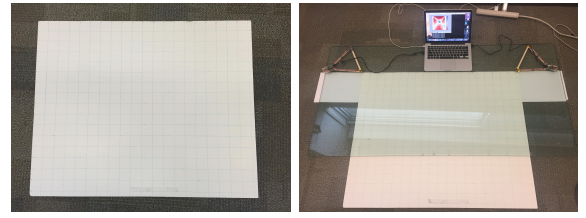
, where $L_1(x, y)$ and $L_2(x, y)$ represents the likelihood map from array 1 and array 2.

To see the effect of using multiple arrays, fig 6 shows the individual likelihood map from each array and also the combined likelihood map according to equation 3. Individual array gives accurate angle estimate, but has high uncertainty in distance estimate. By combining estimates from two arrays, the angle estimate can be effectively combined to estimate distance.

From a timing point of view, the micro-controller spends 12 millisecond on sampling microphone data before sending the data to the computer for processing. Sending data through USB port takes another 18 millisecond, and processing on computer takes around 50 millisecond. Therefore, the total time lag between sound source and localization is around 80 millisecond.

VI. EXPERIMENT RESULTS

To test localization accuracy, an one meter by one meter grid was set up and the arrays are placed at the top left and top right corners of the grid. Fig 7 shows a picture of the setup.



(a) 1 meter by 1 meter grid (b) array placement

Fig. 7: Setup for localization accuracy testing

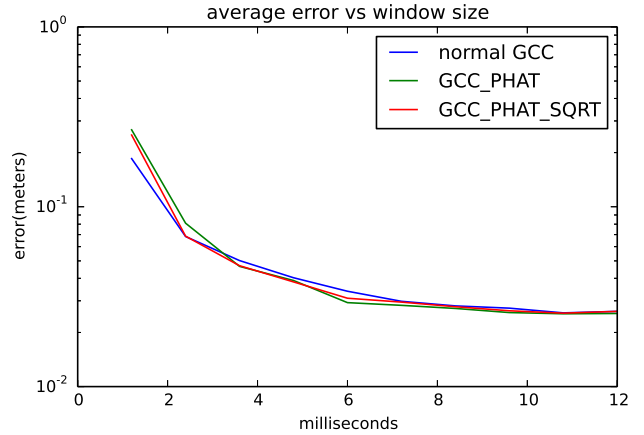


Fig. 8: accuracy versus window size

A total of 32 positions are chosen uniformly in this region where microphone data is recorded. To test how accuracy varies with window size, the algorithm is fed with recorded microphone data with different segment length. Fig 8 shows how accuracy changes with window length for three GCC algorithms. The error lowers as window size increases and plateaus after window size exceeds around 10 millisecond. The lowest error achieved is 2.53 centimeters. It is achieved when window size is set to 12 millisecond and GCC_PHAT is used for TDOA estimation.

Although accuracy improves with window length, the calculation time also increases with window length. The part of calculation that depends on window length is using cross correlation to estimate TDOA. cross correlation can be calculated with FFT and the runtime is of order $O(N \log N)$. We measured how the computation time varies with window length and Figure 9 shows the result. The runtime increases approximately linearly in the window size region of interest.

We also calculated the localization error for each tested point in the region. Figure 10 shows a heatmap of the error distribution inside the grid. The error is below 3 cm for most areas inside the region. There is one error spike in the mid-left region and we contribute this to audio source placement error because the error is fairly low and consistent around that spike region.

To test how well the arrays track movement, we mounted a rotating disk 40 centimeter in diameter onto the grid at

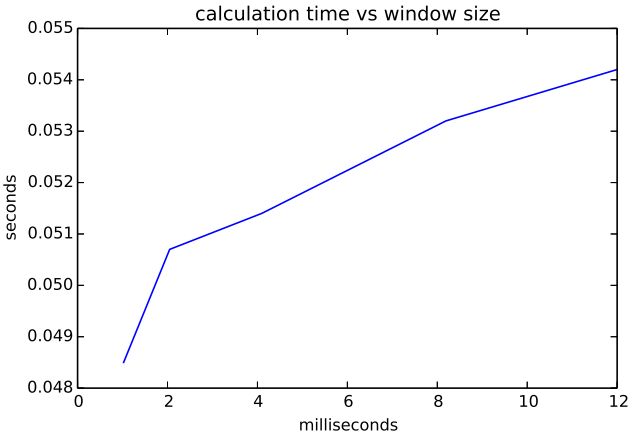


Fig. 9: speed versus window size

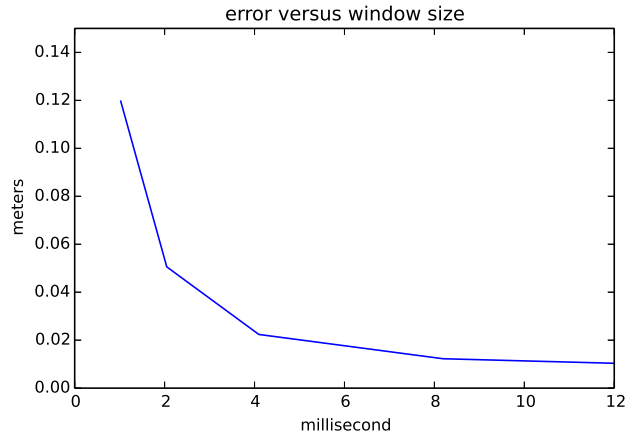


Fig. 13: Localization error versus window size

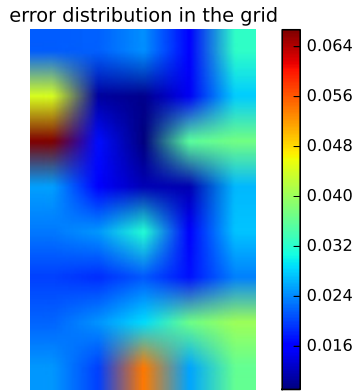


Fig. 10: error distribution in the grid

($x = 0, y = -0.3$). Fig 11 shows a picture of the sestup. A sound source is placed on the edge of rotating disk and the arrays localizes the sound source as it rotates in a circle. In this experiment, we tested how accuracy changes with:

- different window sizes
- different audio sources
- different movement tracking filters
- different movement speeds

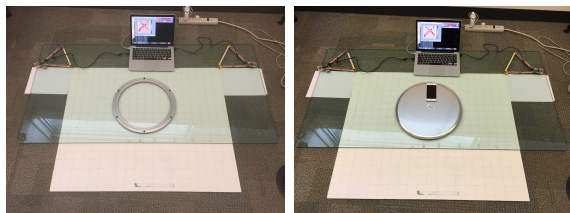


Fig. 11: Setup for circle movement localization

Fig 13 gives an intuitive representation of how accuracy changes with window size. When window size is small(1.02 millisecond), the audio does not contain enough information to reliably estimate TDOA. The localization is noisy. As window size increases, the localization converges to the shape of ground truth circle. Fig 13 shows how the error changes with window size. The general trend is similar to that in point localization case. The error decreases as window size increases and plateaus after window size exceeds around 10 milliseconds.

To test how different sound sources impact localization quality, we conducted three experiments on the same movement track with three different sound sources:

| | |
|-------------|--|
| White Noise | A recording of white noise. |
| Music A | A music that has normal audio amplitude throughout experiment period was chosen. "Honest Eyes" by Black Tide was the music used. |
| Music B | A music with intermittent low amplitude sections was chosen. "Canon" was the music used. |

To test how sound source movement speed affects localization quality, each of three experiments were conducted at two different speeds:

| | |
|--------|--|
| Normal | An angular speed of 0.5 rad/s was maintained, which translates to linear speed of 10 cm/s. |
| Fast | An angular speed of 1.0 rad/s was maintained, which translates to linear speed of 20 cm/s. |

For each experiment conducted, two different movement filters are tests:

| | |
|------------------|--|
| Averaging filter | localization for past 0.5 seconds are averaged and outputed as current estimate. |
| Kalman filter | A 2nd order Kalman filtering is used. |

Fig 14 shows results for experiments with at normal speed, and Fig 15 shows results at fast speed. By comparing localization error for each audio source between normal movement speed and fast movement speed, we find the localization error

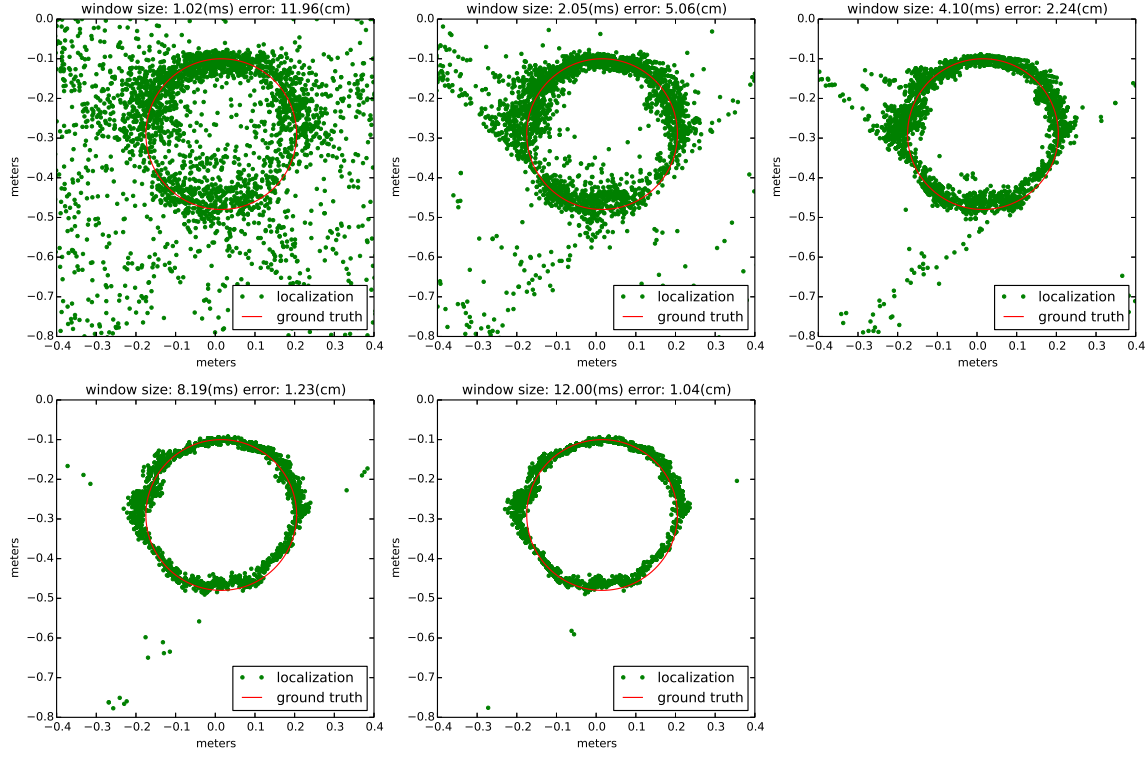


Fig. 12: Localization quality versus window size

does not depend on how fast the sound source is moving. For example fig 14b and fig 15b shows that localization error is 1.289 cm at normal movement speed and 1.291 cm at fast movement speed.

From fig 14, localization error is 0.9 cm for white noise, 1.29 cm for Music A, and 2.9 cm for Music B. Localization accuracy is the best for white noise source, and worst for Music B. This is consistent with our expectation because low amplitude regions in Music B would cause arrays to lose track of where the source is. This can also be seen from the "blank" regions in fig 14c.

Fig 14 also shows that raw detection has the most amount of jiggling. Kalman filter reduces the amount of jiggling from raw detection. Averaging filter has the least amount of jiggling. However, averaging filter averages detection outputs from past 0.5 seconds, which makes the filtered output lag the real movement.

VII. CONCLUSION

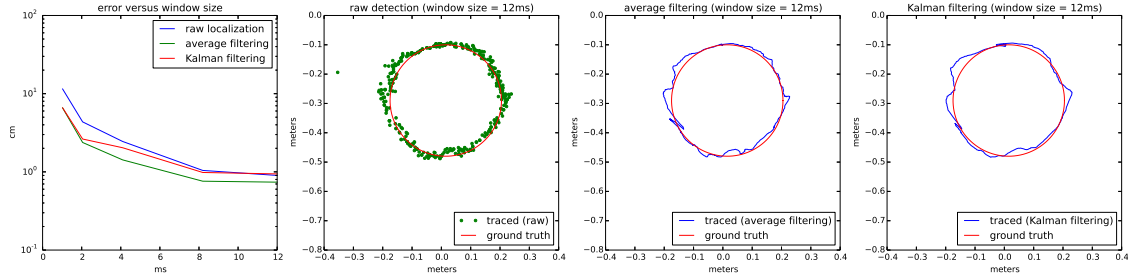
The conclusion goes here.

ACKNOWLEDGMENT

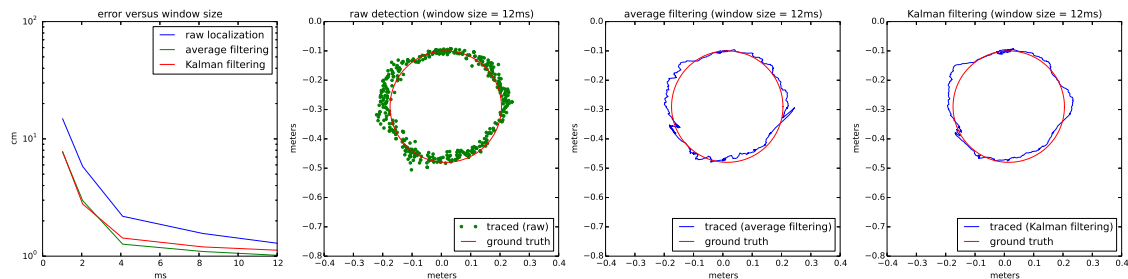
The authors would like to thank...

REFERENCES

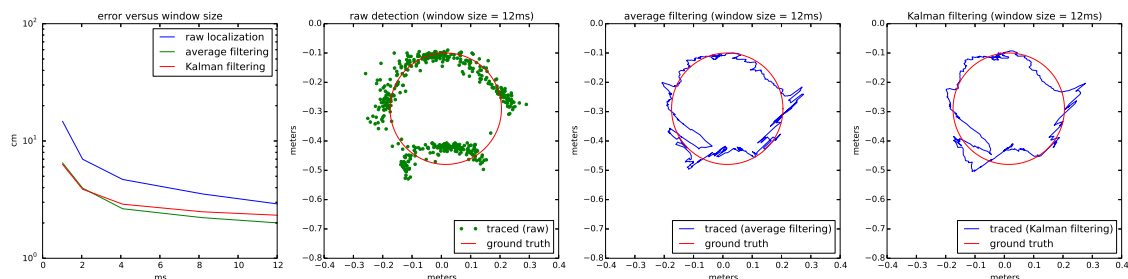
- [1] H. Kopka and P. W. Daly, *A Guide to L^AT_EX*, 3rd ed. Harlow, England: Addison-Wesley, 1999.



(a) white noise

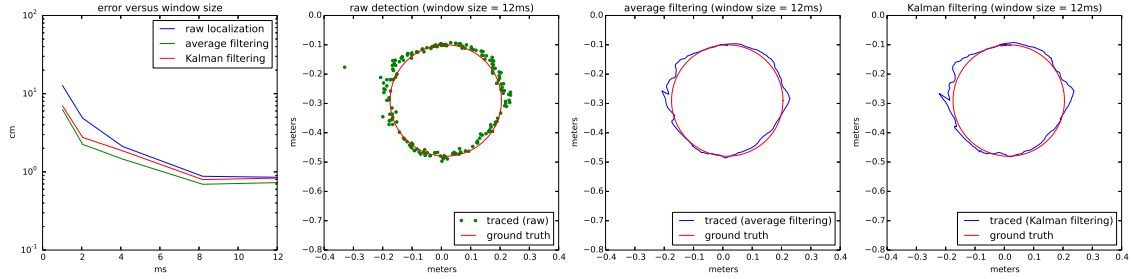


(b) music A

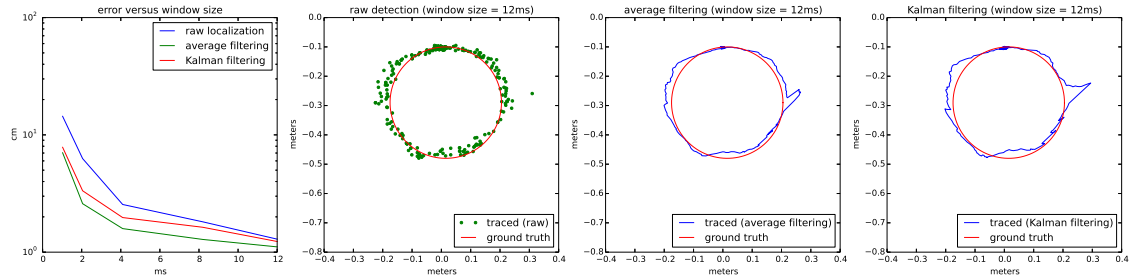


(c) music B

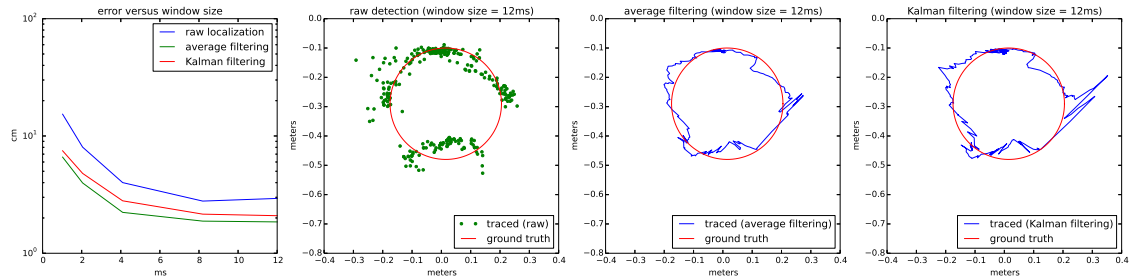
Fig. 14: Localization of circle movement with different sound sources. Sound source is moving at 10 cm per second



(a) white noise



(b) music A



(c) music B

Fig. 15: Localization of circle movement with different sound sources. Sound source is moving at 20 cm per second